

PERFORMANCE AND UPGRADE OF BPMS AT THE J-PARC MR

T. Toyama¹, Y. Hashimoto¹, K. Hanamura³, S. Hatakeyama^{2,3}, M. Okada¹, M. Tejima¹
 J-PARC/KEK¹, J-PARC/JAEA², Mitsubishi Electric System & Service Co.,Ltd³, Tokai, Naka, Japan

Abstract

Since recovery from the great earthquake 2011.3.11, proton beams, more than 10^{14} ppp (protons/pulse), are accelerated up to 30 GeV at the J-PARC MR. For higher intensity beams the following two tasks need to finish: signal attenuation and re-allocation of the BPMS. The attenuator and switchable LPF are attached just before the BPMC (a processing circuit for the BPM). In connection with the MR collimator upgrade to get much more intensity, some BPMS are re-allocated with the steering magnets.

bunch and the bunching factor (B_f) of ~ 0.045 (flat top) are assumed.

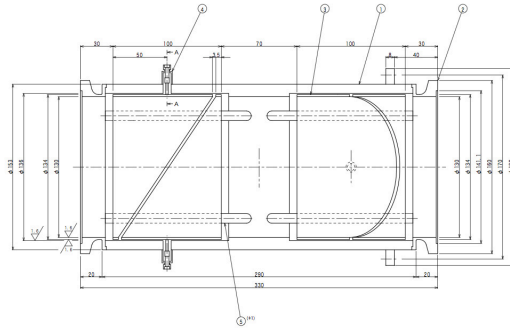


Figure 1: Beam position monitor of the MR.

INTRODUCTION

The BPMS in the J-PARC MR were originally designed with the external capacitors [1, 2]. The aim was to improve a position response by mitigating the capacitive coupling between electrodes, and to get an adequate output voltage at the design intensity, 4×10^{13} ppb (protons/bunch) with the lowered cut-off frequency. However, we decided to abandon the idea of adding the capacitors. With the external capacitors the signal would have been too small at low intensity beams of the initial beam commissioning. On the contrary in the present configuration without capacitors the signal is too large with the design intensity beam. We have added the small box consisted of an attenuator and a switchable LPF just before the BPMC (a processing circuit for the BPM). This paper describes the design and test results on those additional backend-circuits.

To reach higher intensities, we have to admit more controlled beam losses localized at the MR collimator than the original design [3, 4]. The original lattice element order:

Quad. – Drift / Collimator – Steering – [BPM+Quad]

was changed to
 Quad. – Drift / Collimator – Additional collimator – Quad. – [Steering+BPM].

The design and procedure of the re-allocation is reported.

ATTENUATOR PLUS SWITCHABLE LPF FOR MR BPMS

There are 186 BPMS in the MR. A drawing and a photograph of the regular size BPM are depicted in Fig. 1. The electrodes are cut diagonally, which result in linear position response. According with the recent intensity increase, Fig. 2, we need to set the signal attenuators before the present BPMC (Fig.3).

One of the diagonal-cut electrode pair with the inner diameter of $\phi 130$ mm and the length of 100 mm is estimated to produce the signals as shown with a red line in Fig. 3. The design intensity of $\sim 4 \times 10^{13}$ protons per

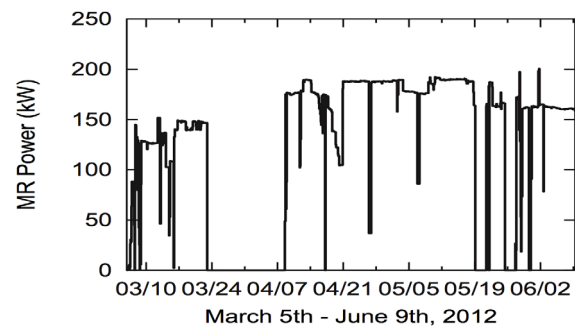


Figure 2: MR beam power history of the fast beam extraction in the first half of FY2012 [5].

Due to the high-pass frequency characteristics of the BPM, higher frequency dominated beam of smaller B_f tends to produce higher BPM output voltage, 108 V at maximum. The peak beam current variation due to adiabatic change of the longitudinal motion during acceleration from 3 GeV to 30 GeV is exaggerated by the high-pass frequency response of the BPM, and the signal variation due to B_f change from 0.3 to 0.045 is ~ 30 times (Fig. 4). Adopting LPF with the cut-off of 796kHz, we obtain the signal voltage for the BPM circuit as 9.25 V at maximum with a 10 dB attenuator as shown in Fig. 3 and 4, which is well below the acceptable input level of the BPM circuits. Moreover the signal voltage variation is reduced to the ratio of ~ 8 .

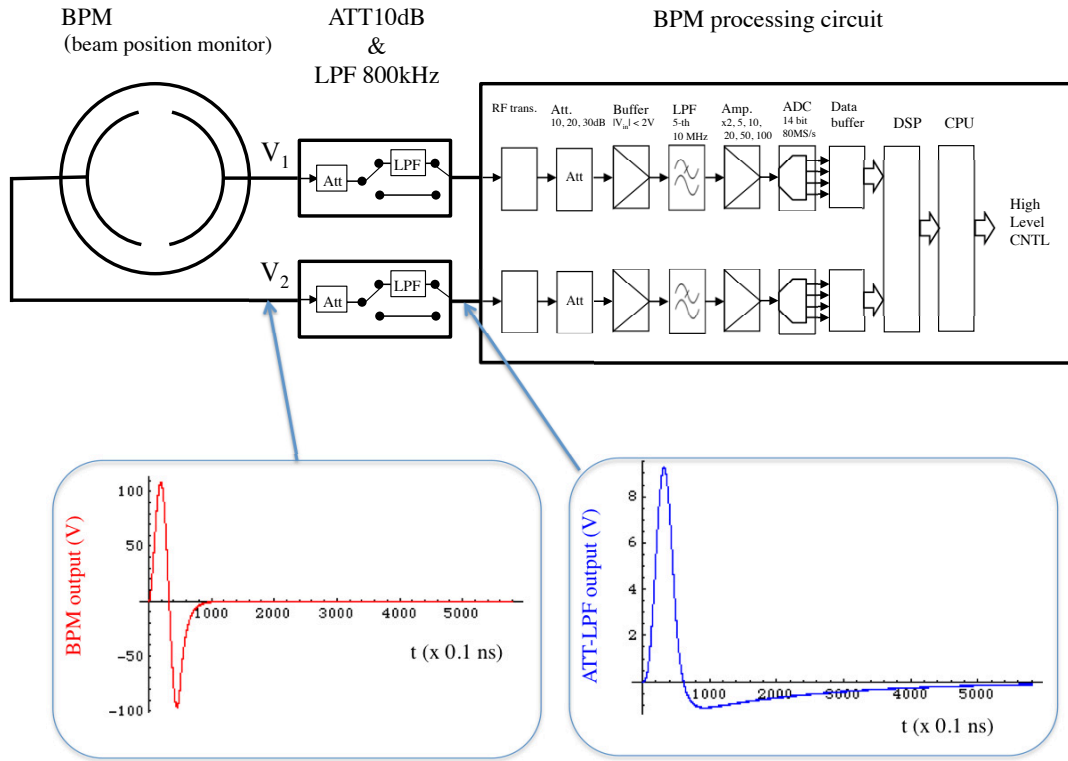


Figure 3: Block diagram and the expected signals.

Copyright © 2013 by JACoW — cc Creative Commons Attribution 3.0 (CC-BY-3.0)

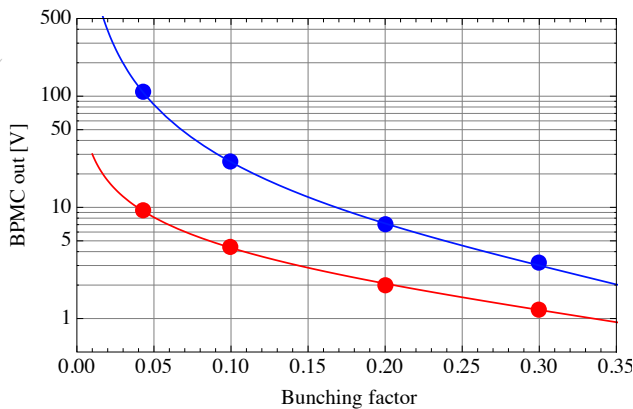


Figure 4: The BPM output voltage (zero-peak) vs. the bunching factor (solid lines as a guide to the eye).

In the frequency domain the combined characteristics of the BPM (Fig. 5, a magenta curve) and the low-pass filter (Fig. 5, a red curve) have a pass-band between 0.73M and 17MHz (Fig. 5, a blue curve). The transition region of the LPF corresponds to the pass band of the combined system. The gain reduction of the LPF needs to be 20 dB/dec for a flat pass band of the combined characteristics. In this sense the LPF works as an equalizer.

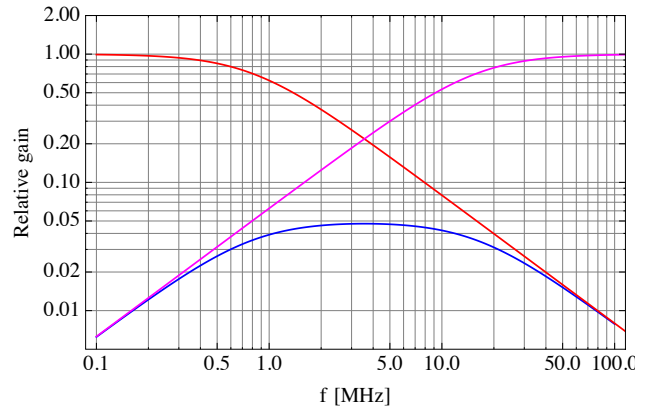


Figure 5: Frequency response of the combined system.

The impedance mismatch at the LPF input with the 50 Ω cable will cause non-negligible reflection. Adding a parallel HPF to the LPF constitutes the all-pass filter that provides good impedance matching. Figure 6 shows the adopted circuit with a cut-off frequency, $f = 796\text{kHz}$. In addition a 10 dB attenuator is attached to attenuate the signal power and to improve the return loss. The measured return loss is more than 53 dB at the detecting frequency of 3.4 MHz for the “COD mode” [1, 2].

Position accuracy is partially governed by the balance of a pair of these filters. The overall accuracy goal is $\Delta x, \Delta y < 0.1$ mm. The goal for the attached ATT-LPF is set at < 0.02 dB (~ 0.2 mm) for each pair. This was done by choosing the pair which satisfies this goal at the detecting frequency of 3.4 MHz. The overall accuracy goal will be met with the “beam-based alignment”.

Linearity of the ATT-LPF was measured with a signal generator (KEITHLEY 3390 [6]), the RF power amplifier (R&K CA010K251-5757R [7]) and the oscilloscope (Tektronix DPO3054 [8]) (Fig. 7). The beam is simulated with the signal generator and RF amplifier. The output of the signal generator is observed with the oscilloscope (Fig. 8 (a)), and amplified with the 57dB RF amplifier. The output signal from the ATT-LPF is shown in Fig. 8 (b). Input/output characteristics are plotted in Fig. 9. Linearity is good within the operating region.

Frequency response was measured with the network analyzer (Agilent Technologies, E5071C [9]). The blue curve in Fig. 10 (a) shows the ATT-LPF input/output characteristics ($|S_{21}|$). The deviation at high frequencies ~ 50 MHz is removed by sharp roll-off of the 5-th order 10 MHz anti-aliasing LPF in the BPMC (Fig. 10 (a), red curve). The calculated HPF response of the BPM is combined with measured characteristics of the ATT-LPF and BPMC in Fig. 10 (b).

The BPMs resolutions are estimated using neighboring three BPMs with beams [10]. The obtained resolutions of horizontal and vertical BPMs are between 20 and 100 μ m rms depending on the installed position along the MR, the beam intensity and the setting of the amplifier / attenuator.

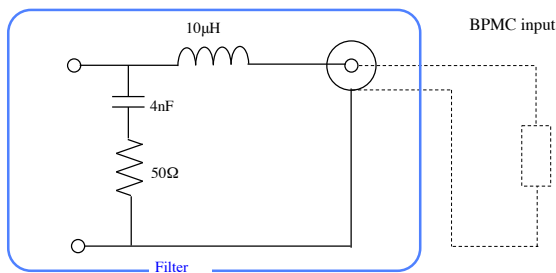


Figure 6: All-pass filter before the BPMC.

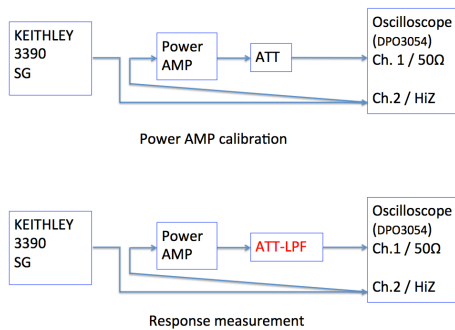
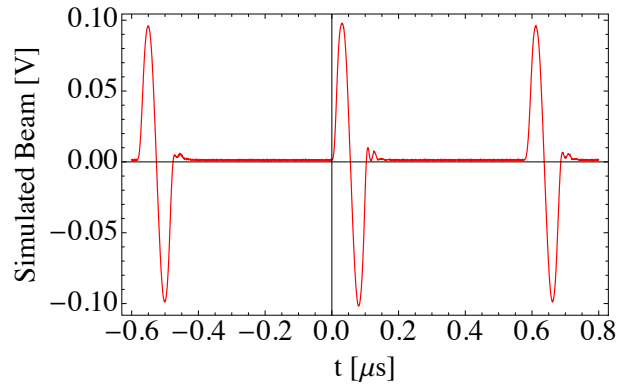
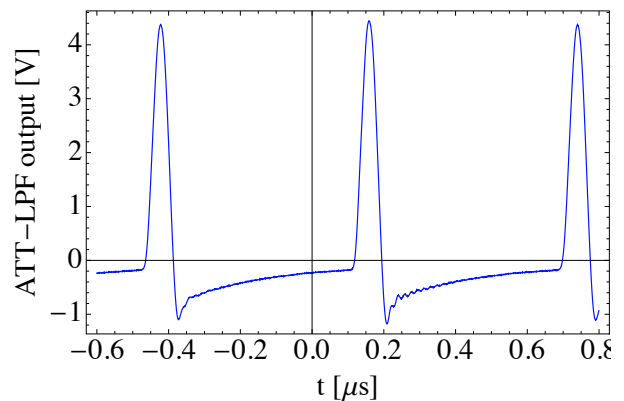


Figure 7: Measurement of the ATT-LPF input/output characteristics.



(a)



(b)

Figure 8: ATT-LPF input/output characteristics. (a) SG output, (b) ATT-LPF output.

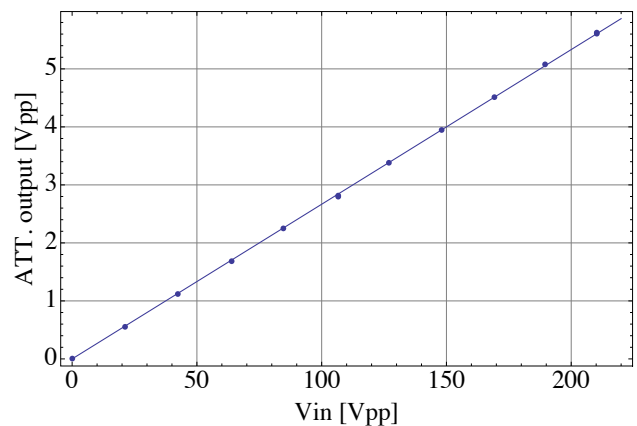


Figure 9: Linearity of the ATT-LPF. (The input is converted to the equivalent BPM output voltage).

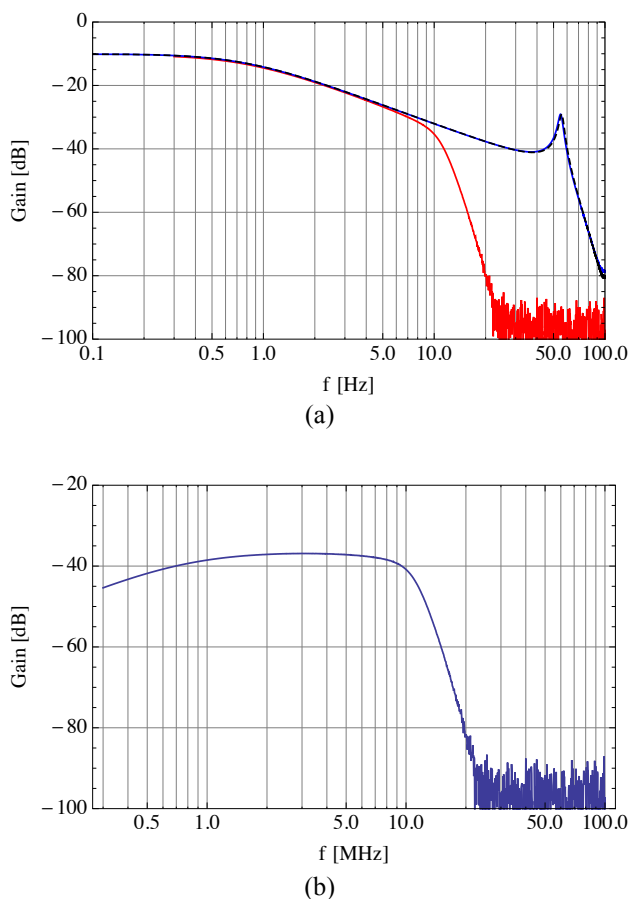


Figure 10: Frequency response of (a) ATT-LPF (blue), ATT-LPF and anti-aliasing LPF (red), and (b) the beam (calculated), ATT-LPF and anti-aliasing LPF.

RECONFIGURATION FOR COLLIMATOR UPGRADE

The “MR collimator” is located at the Insertion-A in the MR [3, 4]. Computer simulations for high intensity proton beams indicates that halo collimation up to ~2 kW at the MR collimator is necessary for more than ~450 kW beam operation. The capacity at the MR collimator is raised from 450 W to 2 kW in 2012 [3, 4]. The layout of beamline elements is changed to accommodate the new collimators.

Previous positions of the #7 and #9 BPMs were located before the quadrupole magnets as shown in Fig. 11 (a). The BPM was held by the support base attached to the end plate of the quadrupole magnet.

The new layout is shown in Fig. 11 (b). The BPM is attached to the steering magnet and makes one rigid structure as a whole. The BPM length was extended from 330 mm to 380 mm to be seen from the laser tracker. Electrodes shape was kept the same as the previous one.

The steering magnets have supports with pins at their bottom. The baseplates with holes were firmly set on the floor [11]. It has the target holes for the laser tracker for survey. The relative positions of the targets were obtained on the basis of the quadrupole coordinate system. The

pair of the BPM and steering magnet was surveyed and aligned to the dummy baseplate with the laser tracker in advance to the installation. This was done at the radiation free area. Installation was very simple because the pins were only put along the holes. This procedure contributed to reduce the sum total of personnel dose. It was about one fifth of the dose for the similar work of FY2011.

The alignment goal was set less than 1 mm. This value corresponds to the range of movement of the bellows. The alignment errors measured by LT were less than 1 mm. The results of beam based alignment (BBA) are shown in Table 1. It also suggests the errors are almost within the goal.

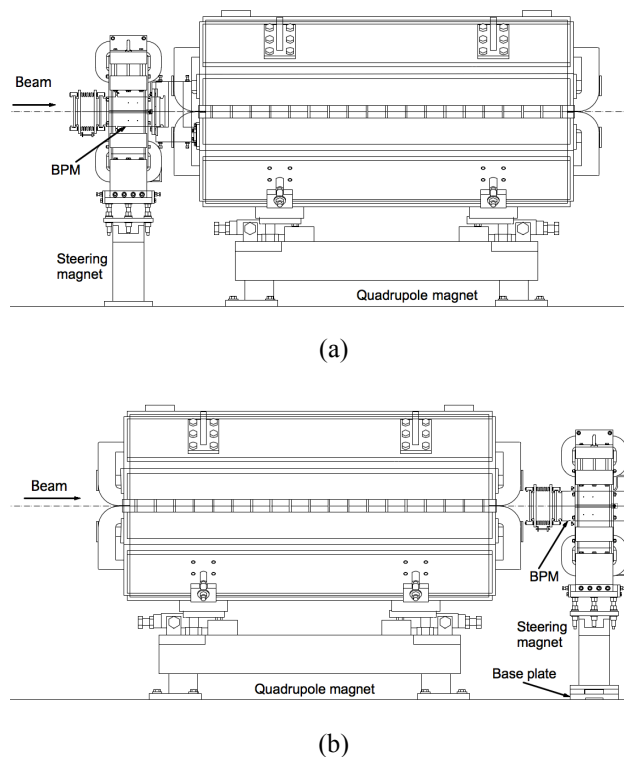


Figure 11: Layout of the BPM, steering and quadrupole magnets (a) before and (b) after reconfiguration.

Table 1: BPM Offset Determined with BBA

	#007 BPM	#009 BPM
Hor. offset	0.56 mm	0.88 mm
Ver. offset	1.15 mm	-0.32 mm

SUMMARY

To achieve higher intensity beam operation more than 450 kW, the following two tasks have been completed successfully.

The ATT-LPFs were attached before the BPMs to attenuate the signals from high intensity beams. The BPMs are presently operated with the beam intensity more than 10^{14} ppp. The position resolutions with these

ATT-LPFs are between 20 and 100 μm rms. In case of low intensity operation of $\sim 4 \times 10^{11}$ ppb as a beam study or beam tuning, LPFs are switched off and we have enough position resolution.

In connection with the MR collimator upgrade to get much more intensity, #7 and #9 BPMs were re-allocated with the steering magnets. Using the dowel pins and holes structure at the steering magnets supports and the base plates on the floor, the installation was drastically simplified. Total personnel dose was much reduced.

ACKNOWLEDGMENT

The authors are indebted to Y.Hori and T.Oogoe for the idea and construction about the dowel pins and holes structure, and to T.Kubota, M.Shirakata, K.Ishii, K.Niki, M.Uota, S.Otsu and K.Onodera for assistance to the design, survey and installation of the BPMs with the steering magnets.

REFERENCES

- [1] T.Toyama, D.Arakawa, R.Toyokawa, A.Nakamura, N. Hayashi and T. Miura, "The BPM Detector for the J-PARC 50 GeV Ring", Proc. of the 14th Symposium on Accelerator Science and Technology, Tsukuba, Japan, 2003, p.470 (in Japanese).
- [2] T. Toyama, D. Arakawa, Y. Hashimoto, S. Lee, T. Miura, and H. Nakagawa, "Beam Position Monitor for the J-PARC Main Ring Synchrotron", Proceedings of DIPAC 2005, Lyon, France.
- [3] J. Takano, K. Ishii, Y. Sato, M. Shirakata, "Simulation Study of Collimators in the J-PARC Main Ring with the STRUCT", Proc. of the 14th Symposium on Accelerator Science and Technology, Tsukuba, Japan, 2012, p.470 (in Japanese).
- [4] T. Koseki, "MR status and study results", ATAC, Tokai, Japan, Feb. 24, 2012.
- [5] Y. Sato, S. Igarashi, M. Shirakata, N. Yamamoto, T. Toyama, M. Tejima, K. Satou, Y. Hashimoto, M. Okada, K. Hara, C. Ohmori, K. Ohmi, K. Ishii, T. Sugimoto, S. Yamada, S. Nakamura, J. Takano, K. Niki, N. Kamikubota, M. Uota, Y. Hori, M. Shimamoto, Y. Kurimoto, M. Yoshii, H. Hotchi, S. Hatakeyama, F. Tamura, T. Koseki, "Recent Commissioning of High-Intensity Proton Beams in J-PARC Main Ring", Proc. of HB2012, Beijing, China (2012) THO1C06.
- [6] <http://www.keithley.com>
- [7] <http://www.rk-microwave.com>
- [8] <http://www.tek.com/>
- [9] www.home.agilent.com
- [10] T. Suwada, N. Kamikubota, H. Fukuma, N. Akasaka, H. Kobayashi, "Stripline-type beam-position-monitor system for single-bunch electron/positron beams", Nucl. Instr. and Meth. A 440 (2000) 307.
- [11] K. Hanamura, T. Toyama, Y. Hashimoto, T. Oogoe, T. Kubota, M. Shirakata, K. Ishii, K. Niki, Y. Hori, M. Uota and S. Otsu, "BPM Installation at the High Radiation Area (J-PARC MR Collimator)", Proc. of the 9th Annual Meeting of Particle Accelerator Society of Japan, Osaka, Japan, 2012 (in Japanese).